catalysts

MDPI

Article

Effects of Promoter's Composition on the Physicochemical Properties of $Cu/ZnO/Al_2O_3$-ZrO_2 Catalyst

Nur Insyirah Zulkifli [1], Noor Asmawati Mohd Zabidi [1,*], Zulkifli Merican Aljunid Merican [1] and Sara Faiz Hanna Tasfy [2]

[1] Center of Contaminant Control and Utilization (CenCoU), Institute of Contaminant Management for Oil and Gas, Department of Fundamental and Applied Sciences, Universiti Teknologi PETRONAS, Seri Iskandar 32610, Perak, Malaysia; nur_19000323@utp.edu.my (N.I.Z.); zulkifli.aljunid@utp.edu.my (Z.M.A.M.)

[2] Department of Chemical and Petroleum Engineering, American University of Ras Al Khaimah, Ras Al Khaimah 10021, United Arab Emirates; sara.tasfy@aurak.ac.ae

* Correspondence: noorasmawati_mzabidi@utp.edu.my; Tel.: +60-5-368-7675

Abstract: Cu/ZnO catalysts were synthesized via an impregnation method on an Al_2O_3-ZrO_2 support and modified by the addition of manganese and niobium as promoters. The effect of the selected promoters on the physicochemical properties and performance toward the hydrogenation of CO_2 to methanol are presented in this paper. The Mn and Nb promoters improved the reducibility of the catalyst as evidenced by the shifting of the H_2-TPR peaks from 315 °C for the un-promoted catalyst to 284 °C for the Mn- and Nb-promoted catalyst. The catalytic performance in a CO_2 hydrogenation reaction was evaluated in a fixed-bed reactor system at 22.5 bar and 250 °C for 5 h. Amongst the catalysts investigated, the catalyst with equal ratio of Mn and Nb promoters exhibited the smallest particle size of 6.7 nm and highest amount of medium-strength basic sites (87 µmol/g), which resulted in the highest CO_2 conversion (15.9%) and methanol selectivity (68.8%).

Keywords: CO_2 hydrogenation; methanol synthesis; manganese; niobium; Cu-based catalyst

Citation: Zulkifli, N.I.; Zabidi, N.A.M.; Merican, Z.M.A.; Tasfy, S.F.H. Effects of Promoter's Composition on the Physicochemical Properties of $Cu/ZnO/Al_2O_3$-ZrO_2 Catalyst. *Catalysts* **2022**, *12*, 636. https://doi.org/10.3390/catal12060636

Academic Editors: Qinghua Lai, Qingfeng Zhang and Run-Ping Ye

Received: 1 May 2022
Accepted: 3 June 2022
Published: 10 June 2022

1. Introduction

The carbon dioxide content in the earth's atmosphere increases significantly due to domestic and industrial activities, such as open burning, use of fossil fuels, and deforestation. According to the National Aeronautics and Space Administration (NASA) [1], the concentration of CO_2 has increased significantly since the mid-19th century and it reached 441 ppm in May 2019. It is reported that in the late 1950s until 2004, the annual rate of the increase in CO_2 concentration was about 0.73 ppm per year. In comparison, from the year 2005 until 2014, the rate shows an increase of about 2.11 ppm per year. In response to this issue, carbon capture and storage technology has been introduced to capture waste carbon dioxide from industries by transporting it to a storage site or converting it into valuable chemicals [2–4].

Accordingly, there has been intense interest in CO_2 valorization either through the adsorption of CO_2 or conversion to valuable products and chemicals [5–10]. In order to meet the increasing demand for energy supply, researchers are exploring the technological challenges in producing methanol via CO_2 hydrogenation as well as the process economy for a methanol plant [11,12]. Methanol is the main precursor to synthesize valuable chemicals for liquid fuel production, such as di-methyl-ether (DME), as well as an alternative oil derivative and several bulk chemicals, e.g., methyl-tert-butyl-ether (MTBE), formaldehyde, and acetic acid.

Methanol is produced industrially from syngas (a mixture of H_2 and CO) using a $Cu/ZnO/Al_2O_3$ conventional catalyst [13]. The conventional $Cu/ZnO/Al_2O_3$ catalyst is preferred in industrial methanol synthesis due to its good catalytic ability, long life

time, and relatively low temperature and pressure reaction conditions [14]. Furthermore, Al-containing precursors produced small CuO crystals with high specific surface area [15]. The Cu-O-Zn acts as the active site for the CO hydrogenation reaction to form methanol via the syngas feedstock [16]. Similar Cu-based catalysts are also being applied for the methanol synthesis process via the CO_2 hydrogenation route where Cu^+ is found to act as the active site in the CO_2 hydrogenation reaction [17].

Table 1 shows some Cu-based catalysts used in methanol synthesis via the CO_2 hydrogenation reaction by several researchers [18–27]. A recent review on promoters for methanol synthesis via CO_2 hydrogenation using a Cu-based catalyst was also presented by Niu et al. [7]. The promoters employed include metals, as well as rare-earth and non-metallic elements. The promoters that are commonly investigated are zirconium, gallium, and magnesium. The presence of these promoters modified the basicity and physicochemical properties of the Cu-based catalysts and enhanced methanol production via the CO_2 hydrogenation reaction. The addition of ZrO_2 in the Cu-based catalyst improved both the CO_2 conversion and methanol selectivity, as depicted in Table 1. Li et al. [24] studied the effect of a Zr-doped Cu-Zn-Zr-Al catalyst and found that added Zr suppressed the inhibitive effect of water for the reaction, and thus prevented catalyst deactivation. The formation of a highly stable catalyst increased the Cu surface areas and led to higher methanol selectivity, compared to that of the un-promoted Cu-Zn-Al catalyst, by 17.3% in terms of the CO_2 hydrogenation activity.

Table 1. Summary of the CO_2 hydrogenation performance of Cu/ZnO-based catalyst in a fixed-bed reactor.

Catalyst	Promoter	T (°C)	P (MPa)	GHSV *	CO_2 Conv. (%)	Selectivity (%)	Ref.
$Cu/ZnO/Al_2O_3$	-	250	5	4000 h^{-1}	20.2	42.3	[18]
$Cu/ZnO/Al_2O_3$	Zr (0.3)	250	5	4000 h^{-1}	22.5	47.4	[18]
Cu/γ-Al_2O_3	-	250	2	1400 h^{-1}	8.98	13.4	[19]
Cu/γ-Al2O3	ZnO, ZrO_2, MgO	250	2	1400 h^{-1}	12.12	35.98	[19]
$Cu/ZnO/Al_2O_3$	-	200	5	260 mL min^{-1} g^{-1}	7.1	78	[20]
$Cu/ZnO/Al_2O_3$	MgO	200	5	260 mL min^{-1} g^{-1}	8.1	87	[20]
$Cu/ZnO/ZrO_2$	-	250	3	61.5 mL min^{-1} g^{-1}	4.08	63.6	[21]
$Cu/ZnO/Al_2O_3$	-	240	2	1350 h^{-1}	4.2	25.8	[22]
$Cu/ZnO/Al_2O_3$	ZrO_2	240	2	1350 h^{-1}	7.4	58.1	[22]
$Cu/ZnO/Al_2O_3$	Ga_2O_3	240	2	1350 h^{-1}	4.4	32.5	[22]
$Cu/ZnO/Al_2O_3$	-	250	5	200 mL min^{-1} g^{-1}	19.7	39.7	[23]
$Cu/ZnO/Al_2O_3$	Mn	250	5	200 mL min^{-1} g^{-1}	22.3	43	[23]
$Cu/ZnO/Al_2O_3$	Zr	250	5	200 mL min^{-1} g^{-1}	24.7	48	[23]
Cu/ZnO	Al_2O_3	230	3	-	18.7	43	[24]
Cu/ZnO	Al_2O_3- ZrO_2	230	3	-	23.2	60.3	[24]
$Cu/ZnO/ZrO_2$	Ga_2O_3	250	8	3300 h^{-1}	-	75	[25]
$Cu/ZnO/Al_2O_3$	-	250	5	10 h^{-1}	4	76	[26]
$Cu/ZnO/Nb_2O_5$	-	250	5	10 h^{-1}	1	100	[26]
Cu/ZnO/SBA15	Nb	250	2	175 mL min^{-1} g^{-1}	17.1	98	[27]

* GHSV is gas hourly space velocity. The feed ratio of H_2:CO_2 = 1:3.

The effects of oxide additives (B, Ga, In, Gd, Y, Mg, and Mn) on the catalytic activity of a $Cu/ZnO/ZrO_2$ catalyst were reported and amongst the additives investigated, the Ga_2O_3 additive resulted in the highest enhancement in the methanol yield from the CO_2 hydrogenation reaction [25]. A similar trend was also reported by Saito [28], Toyir [29], and Xaba [22]. The introduction of Ga^{3+} in the Cu/ZnO catalyst facilitated the reduction of Zn^{2+} to Zn^0 to form a CuZn alloy, which enhanced the performance of the catalyst [30].

Gao et al. [23] reported that the introduction of Mn, La, Ce, Zr, and Y enhanced the BET surface area, Cu surface area, and dispersion, as well the strong basic site portion of the Cu/Zn/Al catalyst, which favors the formation of methanol. The methanol selectivity increased by about 20% and 8%, respectively, over the Zr- and Mn-promoted Cu/Zn/Al catalyst compared to that of the un-promoted catalyst in the CO_2 hydrogenation reaction. Tripathi et al. [31] also reported an increase of 22% in methanol selectivity for the Mn-promoted Cu/Zn -based catalyst compared to that of the unpromoted catalyst using CO_2-rich syngas feedstock. The presence of up to 20 mol% Mn facilitated the maximum dilution of Cu^{2+} ions and modified the microstructures of the catalyst which led to an enhancement in the catalytic activity of the Cu/Zn-based catalyst.

On the other hand, our previous finding indicated that Nb increased the dispersion of the copper catalyst and improved the methanol yield by ~2 folds compared to that of the un-promoted catalyst in a CO_2 hydrogenation reaction over the Cu/ZnO/SBA15 catalyst [27]. Meanwhile, Silva et al. [26] reported that the Nb_2O_5-supported Cu/ZnO catalyst resulted in higher methanol selectivity compared to that of the Cu/ZnO/Al_2O_3 catalyst. The effects of polymorphic ZrO_2 phase as a support for the Cu/ZnO catalyst have been reported recently [32]. The higher methanol yield over the Cu/ZnO catalyst supported on tetragonal phase of ZrO_2 was due to the lower activation energy compared to that supported on ZrO_2 containing a greater amount of monoclinic phase.

Despite numerous investigations of the CO_2 conversion processes, the reaction mechanism and types of active sites for the production of methanol from CO_2 hydrogenation are still debatable. The activation of CO_2 requires high energy input as it exists in its most stable state. The search for better catalysts in CO_2 activation is still a subject of great interest in methanol synthesis. To the best of the authors' knowledge, the effects of Mn and Nb promoters on Cu/Zn/Al_2O_3-ZrO_2 have not been published elsewhere. This study aims to investigate the effect of Mn and Nb promoters on the physicochemical properties of a Cu/ZnO catalyst supported on Al_2O_3-ZrO_2 and its catalytic performance towards the hydrogenation of CO_2 to methanol.

2. Results and Discussion

2.1. Physicochemical Properties

A series of Cu/ZnO catalysts were synthesized on Al_2O_3-ZrO_2 support via the impregnation method. Promoters, such as Mn and Nb, were added to the catalyst. The synthesized samples were characterized in terms of phase, texture, particle size, dispersion, reducibility, and basicity. Characterization of synthesized catalysts was performed using the calcined samples. The XRD profile of the calcined catalyst is illustrated in Figure 1. XRD analysis was conducted to determine the catalyst phase using peak matching with International Centre for Diffraction Data (ICCD) and Inorganic Crystal Structure Database (ICSD). All catalyst samples showed the same diffraction patterns but varied in the intensity of the peaks. The low peak intensity of promoted Cu/ZnO/Al_2O_3-ZrO_2 suggests the presence of a microcrystalline structure. As shown in Figure 1, the XRD profile of the Al_2O_3-ZrO_2 support exhibits four significant peaks at 2θ of 32.1°, 39.5°, 60.9°, and 67.1° (ICSD 03-065-6868), confirming the existence of the monoclinic phase of Al_2O_3-ZrO_2. Monoclinic CuO was detected at 2θ of 35.3°, 39.7°, and 67.1°, while cubic ZnO at 2θ of 37.6° and 67.1° (ICSD 01-070-6827, ICDD 00-013-0311). The crystallinity of the Al_2O_3-ZrO_2 support decreased when CuO and ZnO were impregnated on the support, as shown by the decrease in the intensity of the peak at 2θ = 32.1° in Figure 1 (ii).

The morphology of the calcined (un-reduced) samples of Cu-ZnO/Al_2O_3-ZrO_2 (CZAZ, un-promoted) and double -promoted Cu-ZnO/Al_2O_3-ZrO_2 (Mn:Nb, Mn:2Nb, and 2Mn:Nb) are shown in Figure 2.

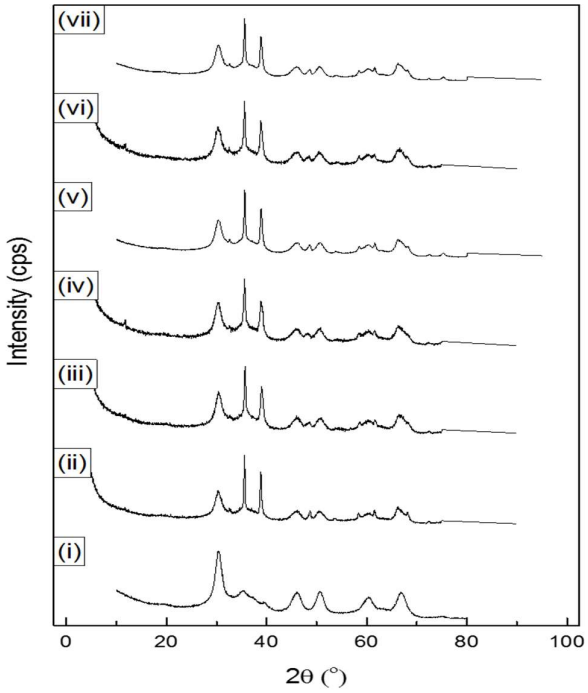

Figure 1. XRD profiles of calcined (un-reduced) samples of (i) Al_2O_3-ZrO_2 support, (ii), un-promoted CZAZ, and promoted Cu/ZnO/Al_2O_3-ZrO_2: (iii) Nb, (iv) Mn, (v) Mn:Nb, (vi) Mn:2Nb, and (vii) 2Mn:Nb.

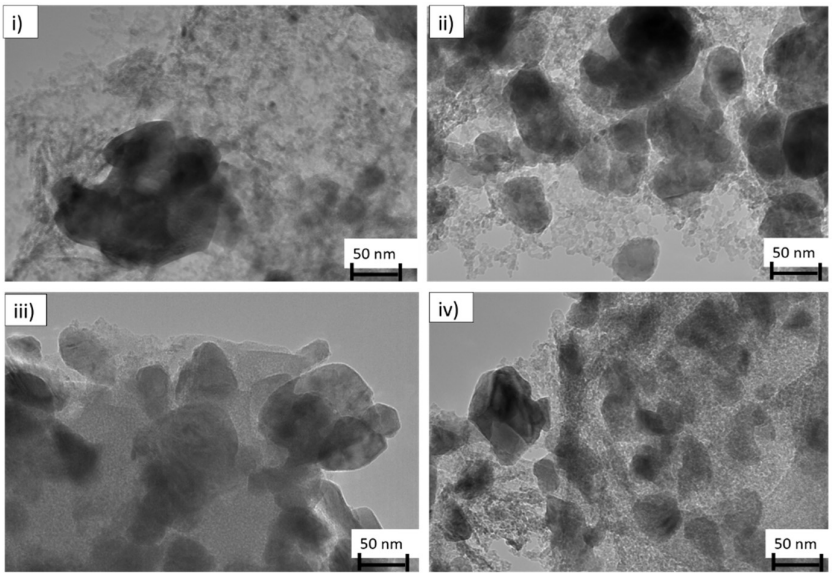

Figure 2. TEM images of calcined (un-reduced) samples for (**i**) un-promoted catalyst (CZAZ), (**ii**) doubly promoted catalyst (Mn/Nb/Cu/ZnO/Al_2O_3-ZrO_2), (**iii**) Mn/2Nb/Cu/ZnO/Al_2O_3-ZrO_2, (**iv**) 2Mn/Nb/Cu/ZnO/Al_2O_3-ZrO_2 at magnification: 200K and scale: 50 nm.

All the catalysts have irregular shape and non-homogenous metal oxide particles. Moreover, the un-promoted catalyst shown in Figure 2 (i) displays agglomerated particles over the surface of the catalyst support. Based on the TEM analysis, the average particle size of the un-promoted CZAZ catalyst was 47.0 nm. Meanwhile, the addition of an equal ratio of Mn:Nb as promoter caused an approximately 86% size reduction as the metal oxide particles significantly reduced from 47.4 nm to 6.7 nm, indicating an increase in the metal interaction due to the addition of the equal ratio of Mn:Nb promoters [33]. On the other hand, the addition of a 1:2 ratio of Mn:Nb also decreased the particle size

from 47.0 nm to 39.4 nm. However, the addition of a 2:1 ratio of Mn:Nb increased the particle size to 51.4 nm, which is 8% larger than that of the un-promoted CZAZ catalyst. Regarding variations in particle size, either smaller or larger particles were influenced by the electronic configurations of the metals when they interact with each other. These electronic configurations varied based on the coordination number, bond length, as well as their packing density [33]. Table 2 shows the average particle size of the catalysts, measured using 30 nanoparticles of each catalyst sample.

Table 2. Average particle size of the calcined catalysts (un-reduced samples).

Catalyst	CuO and ZnO Particle Size (nm)	Standard Deviations (nm)
CZAZ (un-promoted)	47.4	3.4
Mn/Nb/Cu/ZnO/Al_2O_3-ZrO_2	6.7	2.9
Mn/2Nb/Cu/ZnO/Al_2O_3-ZrO_2	51.4	2.8
2Mn/Nb/Cu/ZnO/Al_2O_3-ZrO_2	34.9	3.0

The reducibility of the calcined catalysts was determined by the H_2-TPR technique and their H_2-TPR profiles are presented in Figure 3. Two distinct TPR peaks, denoted as α and β, represent the stepwise reduction behavior of the Cu-based catalysts. The α peak resulted from the reduction of highly dispersed copper species while the β peak is ascribed to the reduction of bulk-like CuO particles [34,35]. López-Suárez et al. also claimed that the α peak corresponds to the easily reduced form of Cu^{2+} and peak β was assigned to the less reducible CuO [36]. The reduction temperature for all the promoted catalysts appeared at lower temperatures compared to those of the un-promoted sample (CZAZ), as shown in Table 3. The impregnation of bimetallic components Cu and ZnO on the Al_2O_3-ZrO_2 support decreased the reduction temperature by 25 °C compared to that of the mono-metallic catalyst of pure bulk CuO, which reduced at 340 °C [17]. The un-promoted CZAZ catalyst only exhibited a β peak corresponding to the presence of only bulk CuO. The presence of reduction profiles with shoulder peaks has also been reported in the literature [34,37]. The singly-promoted catalysts (Nb or Mn) exhibited an α peak at 237–238 °C, contrary to that of the un-promoted catalyst. Similar trends have been obtained for the doubly-promoted, Mn:Nb, Mn:2Nb, and 2Mn:Nb samples, where all the promoted catalyst samples showed the presence of the α and β reduction peaks. The relative contribution of the α peak is the highest (53%) when the catalyst is promoted with a 1:2 Mn:Nb ratio which indicated the higher dispersion of CuO. These TPR profiles indicate that both Nb and Mn promoters improved the reducibility and dispersion of CuO species. The results show that reduction temperatures for the Mn and Nb promoted catalysts occurred between 235 and 296 °C, indicating the presence of CuO species with different degrees of dispersion and/or interaction with other components in the catalyst [17]. The trend in the catalytic reduction obtained from this study agrees with those reported by Ud-din et al. as they also found that Nb_2O_5 significantly improved the reducibility of the Cu/ZrO_2 catalyst [35].

Table 3. H_2-TPR data of catalysts.

Samples	Total H_2 Consumption (μmol/g)	Reduction Temperature (°C)		H_2 Consumption (%)	
		α	β	[α/(α + β) × 100]	[β/(α + β) × 100]
CZAZ (un-promoted)	885	-	315	-	100
Nb/Cu/ZnO/Al_2O_3-ZrO_2	790	237	263	41	59
Mn/Cu/ZnO/Al_2O_3-ZrO_2	907	238	277	23	77
Mn/Nb/Cu/ZnO/Al_2O_3-ZrO_2	1030	284	296	47	53
Mn/2Nb/Cu/ZnO/Al_2O_3-ZrO_2	919	235	275	53	47
2Mn/Nb/Cu/ZnO/Al_2O_3-ZrO_2	1243	243	281	34	66

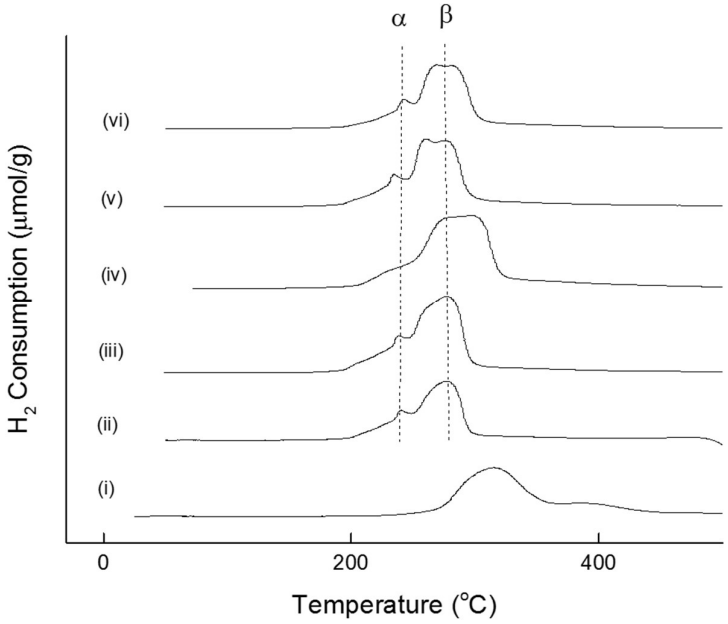

Figure 3. H_2-TPR profiles of (i) un-promoted (CZAZ) and promoted catalysts (ii) Nb/Cu/ZnO/Al_2O_3-ZrO_2, (iii) Mn/Cu/ZnO/Al_2O_3-ZrO_2 (iv) Mn/Nb/Cu/ZnO/Al_2O_3-ZrO_2, (v) Mn/2Nb/Cu/ZnO/Al_2O_3-ZrO_2, and (vi) 2Mn/Nb/Cu/ZnO/Al_2O_3-ZrO_2.

Furthermore, the CO_2 temperature-programmed desorption profiles of the catalysts and a summary of the desorption analysis are presented in Figure 4 and Table 4, respectively. The strength of basic sites is categorized into three groups, low (<200 °C), medium (200–500 °C), and strong (>500 °C). The weak basic sites, T_1 (<200 °C), were assigned to CO_2 species adsorbed onto the weakly held surface hydroxyl groups and the medium basic sites were attributed to adsorption over the metal oxygen pairs, such as Al-O, Zn-O, Mn-O, Nb-O, and Zr-O [38]. On the other hand, the high temperature desorption peaks (above 500 °C) were related to the coordinatively unsaturated O_2- ions (low coordination oxygen atoms) from the partial breakup of metal-oxygen pairs [39]. Irrespective of the type of promoters added, all the catalysts showed the three peaks of low (α), medium (β), and strong basic sites (γ). The Nb-promoted catalyst contained the highest number of strong basic sites (137 µmol/g), whereas the equal ratio Mn:Nb promoted sample had the highest amount of medium-strength basic sites (87 µmol/g).

As shown in Table 4, Nb promoter significantly affects the amount of medium-strength basic sites. With the addition of Nb, the amount of medium-strength basic sites increased by a factor of eight compared to that of the un-promoted sample (CZAZ). Likewise, the addition of Mn promoter also increased the number of medium-strength basic sites by a factor of 3.5 compared to that of the un-promoted catalyst. Amongst the samples analyzed, the equal ratio Mn:Nb promoter contained the highest number of medium-strength basic sites (87 µmol/g). The medium-strength basic sites for all the catalysts were related to metal-oxygen pairs, such as Al-O, Zn-O, Mn-O, Nb-O, Nb-O_2, Nb_2-O_3, and Zr-O, which could function as active sites for the adsorption and activation of acidic CO_2 molecules.

The textural properties of the calcined catalysts are shown in Table 5. The surface area, S_{BET} value of Al_2O_3-ZrO_2 support decreased from 182 to 154 m^2/g for the un-promoted sample (CZAZ), indicating that part of the pores of the Al_2O_3-ZrO_2 support were impregnated and filled with Cu-ZnO particles. For the singly promoted catalyst, the Mn promoter resulted in an increase in the BET surface area (162 m^2/g) and pore volume (0.36 cm^3/g) compared to the un-promoted catalyst. However, an opposite trend was observed for the Nb-promoted sample, which could be due to the plugging of pores of the catalyst support caused by the change in catalyst particle size. Amongst the doubly promoted catalysts, the equal ratio Mn:Nb had the lowest surface area (140 m^2/g), while Mn:2Nb and 2Mn:Nb

samples exhibit similar values of surface areas and pore volumes as that of the singly Mn-promoted catalyst.

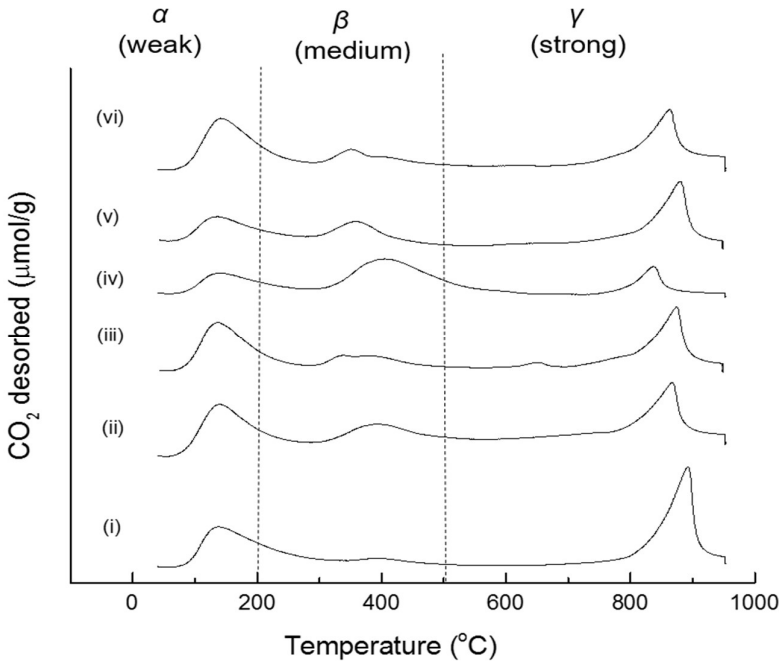

Figure 4. CO_2-TPD profiles of (i) un-promoted (CZAZ) and promoted catalysts (ii) Nb/Cu/ZnO/Al_2O_3-ZrO_2, (iii) Mn/Cu/ZnO/Al_2O_3-ZrO_2 (iv) Mn/Nb/Cu/ZnO/Al_2O_3-ZrO_2, (v) Mn/2Nb/Cu/ZnO/Al_2O_3-ZrO_2, and (vi) 2Mn/Nb/Cu/ZnO/Al_2O_3-ZrO_2.

Table 4. CO_2-TPD data of calcined samples.

Samples	Total Basic Sites (μmol/g)	Peak Temperature (°C)			Number of Basic Sites (μmol/g)		
		T_1	T_2	T_3	α	β	γ
CZAZ (un-promoted)	171	136	392	893	68	10	92
Nb/Cu/ZnO/Al_2O_3-ZrO_2	301	140	391	867	86	78	137
Mn/Cu/ZnO/Al_2O_3-ZrO_2	207	137	339	875	76	36	96
Mn/Nb/Cu/ZnO/Al_2O_3-ZrO_2	151	138	407	834	36	87	29
Mn/2Nb/Cu/ZnO/Al_2O_3-ZrO_2	137	136	357	881	38	27	71
2Mn/Nb/Cu/ZnO/Al_2O_3-ZrO_2	163	141	368	863	79	39	45

The elemental composition of the calcined catalysts was determined using XRF and the results are shown in Table 6. The composition of the synthesized catalysts correlated with theoretical values (70:30 of 15 wt% with promoters loading at 0.09 wt%) with a small deviation in Cu percentages ranging from 0.67 to 0.95%.

Table 5. Textural properties of calcined samples.

Sample	Promoter	S_{BET} (m^2/g)	Vp (cm^3/g)	D_{BJH} (nm)
Al_2O_3-ZrO_2 (support)	-	182	0.38	8.30
CZAZ (un-promoted)	-	154	0.33	6.13
Nb/Cu/ZnO/Al_2O_3-ZrO_2	Nb	134	0.30	6.50
Mn/Cu/ZnO/Al_2O_3-ZrO_2	Mn	162	0.36	6.50
Mn/Nb/Cu/ZnO/Al_2O_3-ZrO_2	Mn:Nb	140	0.31	6.18
Mn/2Nb/Cu/ZnO/Al_2O_3-ZrO_2	Mn:2Nb	162	0.35	6.30
2Mn/Nb/Cu/ZnO/Al_2O_3-ZrO_2	2Mn:Nb	163	0.35	6.30

Table 6. Elemental composition data of calcined samples.

Samples	Weight (%)			
	Cu	**Zn**	**Mn**	**Nb**
Al_2O_3-ZrO_2 (support)	-	-	-	-
CZAZ (un-promoted)	11.24	3.85	-	-
Nb/Cu/ZnO/Al_2O_3-ZrO_2	11.41	3.61	-	0.08
Mn/Cu/ZnO/Al_2O_3-ZrO_2	11.17	3.84	0.08	-
Mn/Nb/Cu/ZnO/Al_2O_3-ZrO_2	11.27	3.72	0.05	0.04
Mn/2Nb/Cu/ZnO/Al_2O_3-ZrO_2	11.45	3.55	0.03	0.05
2Mn/Nb/Cu/ZnO/Al_2O_3-ZrO_2	11.28	3.71	0.04	0.06
		Total: ~15.09%		

Table 7 presents the results of the N_2O chemisorption analysis on the calcined samples. For the un-promoted CZAZ catalyst, the metallic Cu surface area (S_{Cu}) was 6.00 m^2/g, and the Cu dispersion (D_{Cu}) and Cu particle size was 8.87% and 9.80 nm, respectively. Amongst the double-promoted catalysts, the addition of a 2:1 ratio of Mn and Nb promoters resulted in the highest value of Cu surface area S_{Cu} (6.41 m^2/g) and Cu dispersion D_{Cu} (9.48%) compared to those of 1:1 and 1:2 ratio of Mn:Nb. Apart from that, the size of Cu metal (d_{Cu}) was also found to be the smallest (9.16 nm) when Mn:Nb was added at a 2:1 ratio to the catalyst. Moreover, it was observed that the combination of a 1:1 ratio of Mn and Nb resulted in the lowest metallic Cu surface area S_{Cu} (1.87 m^2/g) and Cu dispersion D_{Cu} (2.77%) but the largest size of Cu metal particles (31.3 nm). In comparison with those of other promoter ratios, the lower Cu dispersion might be due to a stronger metal–support interaction in the presence of an equal ratio Mn:Nb promoter, which was also in agreement with the trend observed in the TPR study. Only a small difference in the size of Cu particles was observed for the Mn:2Nb (10.3 nm) and 2Mn:Nb (9.16 nm). The size of metal particles is one of the important parameters in the CO_2 hydrogenation reaction to methanol. Smaller Cu particles are expected to increase the interfacial area of the metal with the neighboring oxide, hence promoting the synergistic effect and improving the performance of the catalyst [39].

Table 7. N_2O chemisorption data of un-promoted and double-promoted CZA catalysts.

Catalyst	Promoter Ratio	Cu Surface Area, S_{Cu} (m^2/g)	Cu Dispersion D_{Cu} (%)	Cu Particle Size, d_{Cu} (nm)
CZAZ	Un-promoted	6.00	8.87	9.80
Mn/Nb/Cu/ZnO/Al_2O_3-ZrO_2	1:1	1.87	2.77	31.3
Mn/2Nb/Cu/ZnO/Al_2O_3-ZrO_2	1:2	5.66	8.37	10.3
2Mn/Nb/Cu/ZnO/Al_2O_3-ZrO_2	2:1	6.41	9.48	9.16

2.2. Catalytic Performance

The performance of the synthesized catalyst in a CO_2 hydrogenation to methanol is shown in Figure 5. The results show that the un-promoted catalyst (CZAZ) exhibits 9.5% CO_2 conversion, 40.8% methanol selectivity, and 3.9% methanol yield, which is lower compared to the performance of the promoted catalysts. The incorporation of a single promoter, namely Mn or Nb, increased the methanol yield to 4.5% and 4.9%, respectively. A notable change in catalytic performance was obtained by combining the Mn and Nb promoters at an equal ratio, which resulted in the highest CO_2 conversion (15.8%), methanol selectivity (68.8%), and methanol yield (10.8%). Amongst the double-promoted catalysts, the equal ratio Mn:Nb promoter exhibited the lowest Cu surface area and Cu dispersion but achieved the highest methanol selectivity in comparison with those of the other ratios. This finding contradicted with the results of Ren et al. [19], whom reported that a ZrO_2-

modified catalyst increased the Cu dispersion and enhanced methanol selectivity. The CO_2 conversion over all catalysts is in the range of 6–16%, which is higher compared to that of palladium-doped $Cu/ZnO/Al_2O_3$ catalyst but similar in terms of methanol selectivity (~64%) [40]. In this work, methanol selectivity over a $Cu/ZnO/Al_2O_3$-ZrO_2 based-catalyst ranged from 40% to 70% due to the formation of by-products, namely methyl formate, methane, and ethanol. The enhancement in CO_2 conversion and methanol selectivity could be due to the availability of a high number of medium-strength basic sites (β peak in the CO_2 TPD profile) in the presence of an equal ratio of Mn and Nb promoters in the catalyst. Amongst the double-promoted catalysts, the Mn:2Nb had the lowest number of medium basic sites (β peak), which also exhibited the lowest catalytic activity. Intermediate species adsorbed on the medium-strength basic sites could preferentially be hydrogenated into methanol as evidenced by the increase in methanol selectivity. The trend in methanol selectivity correlates with the amount of medium-strength basic sites in the catalysts. Our results agree with the findings reported by Guo et al. [20] for a Cu/ZnO-based catalyst where the increase in surface basicity enhanced the adsorption of CO and decreased the methanol adsorption, which led to higher activity and methanol selectivity. The values of CO_2 conversion and methanol selectivity obtained in this work (which used Al_2O_3-ZrO_2 support) are also higher than those reported previously for a similar catalyst composition but supported on Al_2O_3 [19,22,41]. The improvement in catalytic performance might also be contributed by the presence of ZrO_2 (20 wt.%) in the Al_2O_3-ZrO_2 support.

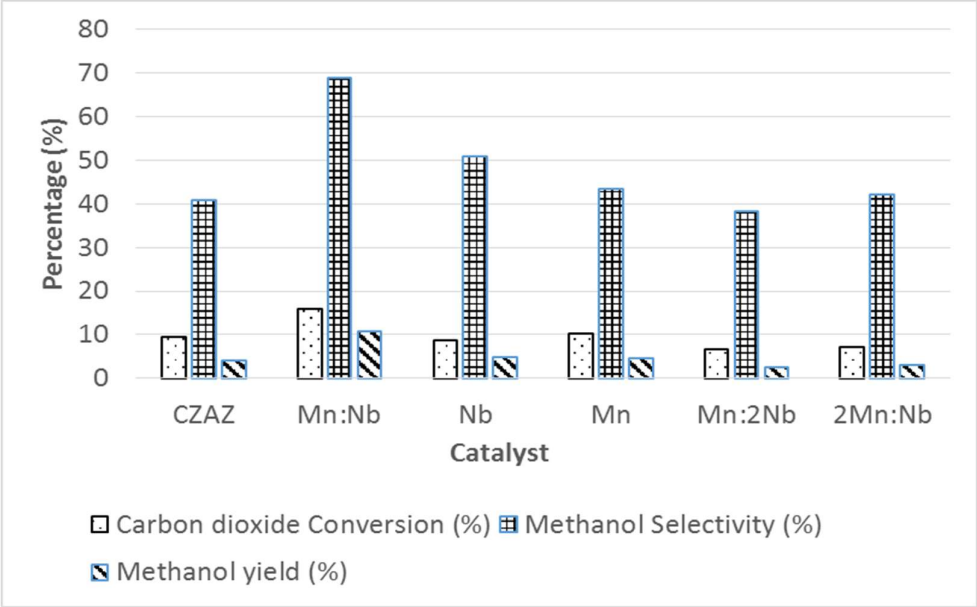

Figure 5. Performance of catalysts at reaction temperature of 250 °C, pressure of 22.5 bar, CO_2:H_2 (1:3) and GHSV of 10,800 mL g^{-1} h^{-1}.

3. Materials and Methods

3.1. Catalyst Synthesis

The catalyst was prepared using an impregnation method with 15 wt.% of metal loading at a Cu to ZnO ratio of 7:3 on a commercial Al_2O_3-ZrO_2 (Sasol, Hamburg, Germany) support. Promoter loading was kept at 0.09 wt.% and the ratio of Mn:Nb promoter was varied from 0 to 2. For the production of 10g of the catalyst, 0.021 g of $Mn(NO_3)_2.4H_2O$ (Merck), 0.014g niobium $C_4H_4NNbO_9$ (Merck, Petaling Jaya, Malaysia), 3.995 g of copper nitrate, $Cu(NO_3)_2$ (Merck), and 1.644 g of zinc nitrate, $Zn(NO_3)_2$ (Sigma Aldrich, Subang Jaya, Malaysia) were dissolved in deionized water and then added to Al_2O_3-ZrO_2 (Sasol, Hamburg, Germany) powder in a dropwise manner. The mixture was continuously stirred for 24 h and the pH was maintained at 7 using 10% ammonia solution, NH_4OH (Merck).

Then, the mixture was filtered and washed using deionized water. The sample was dried at 120 °C for 12 h and calcined in air at 350 °C for 4 h.

3.2. Catalyst Evaluation

Catalyst evaluation was performed in a fixed-bed reactor (Microactivity Reference, PID Eng & Tech, Norcross, GA, USA). Prior to the hydrogenation reaction, 0.2g of calcined catalyst was placed in a stainless-steel tube reactor (I.D = 9 mm, length= 305 mm) and reduced in pure H_2 gas flowing at 20 mL min^{-1} for 2 h at 300 °C. The CO_2 hydrogenation reaction was performed at 22.5 bar, 250 °C, 1:3 CO_2/H_2 ratio, gas hourly space velocity (GHSV): 10,800 mL g^{-1} h^{-1}, and a total feed flow rate of 36 mL min^{-1} for 5 h. The reactor effluents were analyzed on-line using a gas chromatograph (Agilent 7890A, New Castle, DE, USA) equipped with a TCD detector for analyzing H_2 and CO_2 and a FID detector for the quantification of alcohols and other hydrocarbons [27]. The CO_2 conversion and alcohol selectivity were calculated using Equations (1) and (2), respectively.

$$CO_2 \text{ conversion } (\%) = \frac{\text{Mole of } CO_2 \text{ in } - \text{ Mole of } CO_2 \text{ out}}{\text{Mole of } CO_2 \text{ in}} \times 100 \quad (1)$$

$$\text{Methanol selectivity } (\%) = \frac{\text{Mole of methanol produced}}{\text{Total mole of product}} \times 100 \quad (2)$$

3.3. Catalyst Characterization

For phase investigation, an X-ray diffraction (XRD) D2 Phaser from Bruker AXS, GmbH, Germany was utilized, and the phase identifications were determined via PANanalytical High Score Plus software. The XRD profiles were measured at room temperature using a 2θ Bragg angle ranging from 10° to 80°. The TEM analysis for the supported Cu/ZnO-based catalysts was conducted using Zeiss (Jena, Germany) LIBRA 200 FE equipment operated at an accelerating voltage of 200 kV. The reduction profiles of the catalysts were obtained via the hydrogen temperature-programmed reduction (H_2-TPR) using TPR equipment (1100 CE Instrument). Typically, 40–50 mg catalyst was placed in the quartz tube and pre-treated by heating the sample at a ramping rate of 10 °C/min to 250 °C under the flow of pure N_2 for 1 h to remove impurities and moisture. The analysis was then performed by switching the gas flow to 5% H_2/Ar (20 mL/min) and heating to 990 °C at a rate of 10 °C/min for an hour. The carbon dioxide temperature-programmed desorption experiments (CO_2-TPD) were conducted using the same instrument as that of the H_2-TPR experiments. The CO_2-TPD experiments were carried out by placing 40–50 mg of the calcined sample in the quartz tube and pretreating at 250 °C under He flow (20 mL/min) for an hour. The CO_2 sorption then continued by flowing CO_2 at 10 mL/min for 30 min at 75 °C. The desorption of CO_2 was conducted by purging He gas at a flow rate of 20 mL/min through the sorbent bed and ramping the temperature from 40 °C to 950 °C at 10 °C/min. Micromeritics ASAP 2020 (Norcross, GA, USA) at −196 °C was used to determine the BET surface area. In this characterization method, 0.3 g of catalyst was degassed at 300 °C prior to the sorption measurement. The elemental compositions of the samples were determined using the X-ray fluorescence method by placing 3.0 g of calcined sample in the sample holder of the XRF instrument (Bruker AXS S4 Pioneer X-ray Spectrometer, GmbH, Germany). N_2O pulse chemisorption analysis was performed using Micromeritics Autochem II 2920. In this method, temperature was ramped to 260 °C for 1 h under the flow of helium gas at 20 mL/min. The gas flow then changed to H_2 to reduce the CuO before N_2O pulse chemisorption. Temperature was then ramped to 300 °C at 10 °C/min for the duration of 60 min. Temperature was ramped again to 400 °C at 10 °C/min for the duration of 60 min. Finally, temperature was ramped to 500 °C at 10 °C/min for the duration of 60 min. Gas flow was then changed back to helium after a reduction and purge for 30 min, and the temperature was ramped back to 300 °C. Pulse chemisorption began by filling loop gas (loop volume = 0.495 cm^3) with N_2O. The loop gas

(N_2O) was injected into the sample and the dose was repeated for 20 pulses. Finally, the temperature was ramped back to room temperature.

4. Conclusions

The Mn and Nb promoters altered the textural properties, reducibility, and basicity of the $Cu/ZnO/Al_2O_3$-ZrO_2 catalyst and its catalytic performance in the methanol synthesis. Single-promoted Mn or Nb and double-promoted Mn and Nb at three ratios (Mn:Nb, Mn:2Nb, and 2Mn:Nb) for the $Cu/ZnO/Al_2O_3$-ZrO_2 catalysts were synthesized, characterized, and evaluated in methanol synthesis. The Mn and Nb promoters improved the reducibility of the catalysts, as indicated by the H_2-TPR study. Amongst the double-promoted catalysts, the equal ratio of Mn:Nb sample exhibited the highest number of medium-strength basic sites, which resulted in the highest CO_2 conversion (15.9%) and methanol selectivity (68.8%).

Author Contributions: Conceptualization, N.A.M.Z. and S.F.H.T.; methodology, N.I.Z.; formal analysis, N.I.Z.; investigation, N.I.Z.; writing—original draft preparation, N.I.Z.; writing-review and editing, N.A.M.Z., S.F.H.T. and Z.M.A.M.; supervision, N.A.M.Z. and Z.M.A.M.; project administration, N.A.M.Z.; funding acquisition, N.A.M.Z. and S.F.H.T. All authors have read and agreed to the published version of the manuscript.

Funding: This research was funded by International Collaborative Research Fund, (Cost center: 015ME0-207) provided by the Universiti Teknologi PETRONAS and American University of Ras Al Khaimah.

Data Availability Statement: Not applicable.

Acknowledgments: Research support received from Universiti Teknologi PETRONAS and American University of Ras Al Khaimah are gratefully acknowledged (cost center: 015ME0-207).

Conflicts of Interest: The authors declare no conflict of interest.

References

1. NASA. Global Climate Change. Carbon Dioxide Concentration. 2019. Available online: https://climate.nasa.gov/vital-signs/carbon-dioxide/ (accessed on 13 December 2020).
2. Saravanan, A.; Kumar, P.S.; Vo, D.-V.N.; Jeevanantham, S.; Bhuvaneswari, V.; Narayanan, V.A.; Yaashikaa, P.; Swetha, S.; Reshma, B. A comprehensive review on different approaches for CO_2 utilization and conversion pathways. *Chem. Eng. Sci.* **2021**, *236*, 116515. [CrossRef]
3. Kim, S.; Kim, Y.; Oh, S.-Y.; Park, M.-J.; Lee, W.B. Direct utilization of CO_2 via methanol synthesis for natural gas fields with high CO_2 concentration. *J. Nat. Gas Sci. Eng.* **2021**, *96*, 104308. [CrossRef]
4. Atsbha, T.A.; Yoon, T.; Seongho, P.; Lee, C.-J. A review on the catalytic conversion of CO_2 using H_2 for synthesis of CO, methanol, and hydrocarbons. *J. CO2 Util.* **2020**, *44*, 101413. [CrossRef]
5. Goeppert, A.; Olah, G.A.; Surya Prakash, G.K. Toward, a Sustainable Carbon Cycle: The Methanol Economy. In *Green Chemistry: An Inclusive Approach*; Török, B., Dransfield, T., Eds.; Elsevier: Amsterdam, The Netherlands, 2018; pp. 919–962.
6. Biswal, T.; Shadangi, K.P.; Sarangi, P.K.; Srivastava, R.K. Conversion of carbon dioxide to methanol: A comprehensive review. *Chemosphere* **2022**, *298*, 134299. [CrossRef]
7. Niu, J.; Liu, H.; Jin, Y.; Fan, B.; Qi, W.; Ran, J. Comprehensive review of Cu-based CO_2 hydrogenation to CH_3OH: Insights from experimental work and theoretical analysis. *Int. J. Hydrogen Energy* **2022**, *47*, 9183–9200. [CrossRef]
8. Guil-López, R.; Mota, N.; Llorente, J.; Millán, E.; Pawelec, B.; Garcia, R.; Fierro, J.L.G.; Navarro, R.M. Structure and activity of Cu/ZnO catalysts co-modified with aluminium and gallium for methanol synthesis. *Catal. Today* **2020**, *355*, 870–881. [CrossRef]
9. Guil-López, R.; Mota, N.; Llorente, J.; Millán, E.; Pawelec, B.; Fierro, J.L.G.; Navarro, R.M. Methanol Synthesis from CO_2: A Review of the Latest Developments in Heterogeneous Catalysis. *Materials* **2019**, *12*, 3902. [CrossRef]
10. Bhardwaj, R.; Sharma, T.; Nguyen, D.D.; Cheng, C.K.; Lam, S.S.; Xia, C.; Nadda, A.K. Integrated catalytic insights into methanol production: Sustainable framework for CO_2 conversion. *J. Environ. Manag.* **2021**, *289*, 112468. [CrossRef]
11. Alsuhaibani, A.S.; Afzal, S.; Challiwala, M.; Elbashir, N.O.; El-Halwagi, M.M. The impact of the development of catalyst and reaction system of the methanol synthesis stage on the overall profitability of the entire plant: A techno-economic study. *Catal. Today* **2020**, *343*, 191–198. [CrossRef]
12. Cordero-Lanzac, T.; Ramirez, A.; Navajas, A.; Gevers, L.; Brunialti, S.; Gandía, L.M.; Aguayo, A.T.; Sarathy, S.M.; Gascon, J. A techno-economic and life cycle assessment for the production of green methanol from CO_2: Catalyst and process bottlenecks. *J. Energy Chem.* **2022**, *68*, 255–266. [CrossRef]

13. Rahmatmand, B.; Rahimpour, M.R.; Keshavarz, P. Introducing a novel process to enhance the syngas conversion to methanol over Cu/ZnO/Al_2O_3 catalyst. *Fuel Process. Technol.* **2019**, *193*, 159–179. [CrossRef]
14. Bowker, M.; Hadden, R.A.; Houghton, H.; Hyland, J.N.K.; Waugh, K.C. The Mechanism of Methanol Synthesis on Copper/Zinc Oxide/Alumina Catalysts. *J. Catal.* **1998**, *109*, 263–273. [CrossRef]
15. Zhang, F.; Liu, Y.; Xu, X.; Yang, P.; Miao, P.; Zhang, Y.; Sun, Q. Effect of Al-containing precursors on Cu/ZnO/Al_2O_3 catalyst for methanol production. *Fuel Process. Technol.* **2018**, *178*, 148–155. [CrossRef]
16. Choi, Y.; Futagami, K.; Fujitani, T.; Nakamura, J. The difference in the active sites for CO_2 and CO hydrogenations on Cu/ZnO-based methanol synthesis catalysts. *Catal. Lett.* **2001**, *73*, 27–31. [CrossRef]
17. Dasireddy, V.D.; Likozar, B. The role of copper oxidation state in Cu/ZnO/Al_2O_3 catalysts in CO_2 hydrogenation and methanol productivity. *Renew. Energy* **2019**, *140*, 452–460. [CrossRef]
18. Gao, P.; Li, F.; Zhan, H.; Zhao, N.; Xiao, F.; Wei, W.; Zhong, L.; Wang, H.; Sun, Y. Influence of Zr on the performance of Cu/Zn/Al/Zr catalysts via hydrotalcite-like precursors for CO_2 hydrogenation to methanol. *J. Catal.* **2013**, *298*, 51–60. [CrossRef]
19. Ren, H.; Xu, C.; Zhao, H.; Wang, Y.; Liu, J.; Liu, J. Methanol synthesis from CO_2 hydrogenation over Cu/g-Al_2O_3 catalysts modified by ZnO, ZrO_2 and MgO. *J. Ind. Eng. Chem.* **2015**, *28*, 261–267. [CrossRef]
20. Guo, T.; Guo, Q.; Li, S.; Hu, Y.; Yun, S.; Qian, Y. Effect of surface basicity over the supported Cu-ZnO catalysts on hydrogenation of CO_2 to methanol. *J. Catal.* **2022**, *407*, 312–321. [CrossRef]
21. Marcosa, F.C.F.; Lin, L.; Betancourt, L.E.; Senanayake, S.D.; Rodriguez, J.A.; Assaf, J.M.; Giudici, R.; Assaf, E.M. Insights into the methanol synthesis mechanism via CO_2 hydrogenation over Cu-ZnO-ZrO_2 catalysts: Effects of surfactant/Cu-Zn-Zr molar ratio. *J. CO2 Util.* **2020**, *41*, 1012015. [CrossRef]
22. Xaba, B.; Mahomed, A.; Friedrich, H. The effect of CO_2 and H_2 adsorption strength and capacity on the performance of Ga and Zr modified Cu-Zn catalysts for CO_2 hydrogenation to methanol. *J. Environ. Chem. Eng.* **2021**, *9*, 104834. [CrossRef]
23. Gao, P.; Li, F.; Zhao, N.; Xiao, F.; Wei, W.; Zhong, L.; Sun, Y. Influence of modifier (Mn, La, Ce, Zr and Y) on the performance of Cu/Zn/Al catalysts via hydrotalcite-like precursors for CO_2 hydrogenation to methanol. *Appl. Catal. A Gen.* **2013**, *468*, 442–452. [CrossRef]
24. Li, C.; Yuan, X.; Fujimoto, K. Development of highly stable catalyst for methanol synthesis from carbon dioxide. *Appl. Catal. A Gen.* **2014**, *469*, 306–311. [CrossRef]
25. Słoczyn´ski, J.; Grabowski, R.; Olszewski, P.; Kozłowska, A.; Stoch, J.; Lachowska, M.; Skrzypek, J. Effect of metal oxide additives on the activity and stability of Cu/ZnO/ZrO_2 catalysts in the synthesis of methanol from CO_2 and H_2. *Appl. Catal. A Gen.* **2006**, *310*, 127–137. [CrossRef]
26. Da Silva, R.J.; Pimentel, A.F.; Monteiro, R.S.; Mota, C. Synthesis of methanol and dimethyl ether from the CO_2 hydrogenation over CuZnO supported on Al_2O_3 and Nb_2O_5. *J. CO2 Util.* **2016**, *15*, 83–88. [CrossRef]
27. Zabidi, N.A.M.; Tasfy, S.; Shaharun, M.S. Effects of Nb Promoter on the Properties of Cu/ZnO/SBA-15 Catalyst and Performance in Methanol Production. *Key Eng. Mater.* **2016**, *708*, 94–97. [CrossRef]
28. Saito, M.; Fujitani, T.; Takeuchi, M.; Watanabe, T. Development of copper/zinc oxide-based multicomponent catalysts for methanol synthesis from carbon dioxide and hydrogen. *Appl. Catal. A Gen.* **1996**, *138*, 311–318. [CrossRef]
29. Toyir, J.; Piscina, P.R.; Fierro, J.L.G.; Homsa, N. Highly effective conversion of CO_2 to methanol over supported and promoted copper-based catalysts: Influence of support and promoter. *Appl. Catal. B Environ.* **2001**, *29*, 207–215. [CrossRef]
30. Li, M.M.-J.; Zeng, Z.; Liao, F.; Hong, X.; Tsang, S.C.E. Enhanced CO_2 hydrogenation to methanol over CuZn nanoalloy in Ga modified Cu/ZnO catalysts. *J. Catal.* **2016**, *343*, 157–167. [CrossRef]
31. Tripathi, K.; Gupta, V.; Pant, K.K.; Upadhyayula, S. Deciphering Mn modulated structure-activity interplay and rational sta-tistical analysis for CO_2 rich syngas hydrogenation to clean methanol. *J. Clean. Prod.* **2022**, *340*, 130794. [CrossRef]
32. Marcos, F.C.F.; Cavalcanti, F.M.; Petrolini, D.D.; Lin, L.; Betancourt, L.E.; Senanayake, S.D.; Rodriguez, J.A.; Assaf, J.M.; Giudici, R.; Assaf, E.M. Effect of operating parameters on H_2/CO_2 conversion to methanol over Cu-Zn oxide supported on ZrO_2 polymorph catalysts: Characterization and kinetics. *Chem. Eng. J.* **2022**, *427*, 130947. [CrossRef]
33. Zhang, W.B.; Liu, J.; Lu, S.H.; Zhang, H.; Wang, H.; Wang, X.D.; Cao, Q.P.; Zhang, D.X.; Jiang, J.Z. Size effect on atomic structure in low-dimensional Cu-Zr amorphous systems. *Sci. Rep.* **2017**, *7*, 7291. [CrossRef] [PubMed]
34. Koh, M.K.; Wong, Y.; Chai, S.P.; Mohamed, A.R. Carbon dioxide hydrogenation to methanol over multi-functional catalyst: Effects of reactants adsorption and metal-oxide(s) interfacial area. *J. Ind. Eng. Chem.* **2018**, *62*, 156–165. [CrossRef]
35. Din, I.U.; Shaharun, M.; Subbarao, D.; Naeem, A.; Hussain, F. Influence of niobium on carbon nanofibres based Cu/ZrO_2 catalysts for liquid phase hydrogenation of CO_2 to methanol. *Catal. Today* **2016**, *259*, 303–311. [CrossRef]
36. Lopez-Suarez, F.E.; Bueno-López, A.; Illán-Gómez, M. Cu/Al_2O_3 catalysts for soot oxidation: Copper loading effect. *Appl. Catal. B Environ.* **2008**, *84*, 651–658. [CrossRef]
37. Li, F.; Zhan, H.; Zhao, N.; Xiao, F. CO_2 hydrogenation to methanol over La-Mn-Cu-Zn-O based catalysts derived from perovskite precursors. *Int. J. Hydrogen Energy* **2017**, *42*, 20649–20657. [CrossRef]
38. Wu, G.; Wang, X.; Wei, W.; Sun, Y. Fluorine-modified Mg–Al mixed oxides: A solid base with variable basic sites and tunable basicity. *Appl. Catal. A Gen.* **2010**, *377*, 107–113. [CrossRef]
39. Ren, S.; Fan, X.; Shang, Z.; Shoemaker, W.R.; Ma, L.; Wu, T.; Li, S.; Klinghoffer, N.B.; Yu, M.; Liang, X. Enhanced catalytic performance of Zr modified CuO/ZnO/Al_2O_3 catalyst for methanol and DME synthesis via CO_2 hydrogenation. *J. CO2 Util.* **2019**, *36*, 82–95. [CrossRef]

40. Trifan, B.; Lasobras, J.; Soler, J.; Herguido, J.; Menéndez, M. Modifications in the composition of $CuO/ZnO/Al_2O_3$ catalyst for the synthesis of methanol by CO_2 Hydrogenation. *Catalysts* **2021**, *11*, 774. [CrossRef]
41. Tursunov, O.; Kustov, L.; Tilyabaev, Z. Methanol synthesis from the catalytic hydrogenation of CO_2 over CuO–ZnO supported on aluminum and silicon oxides. *J. Taiwan Inst. Chem. Eng.* **2017**, *78*, 416–422. [CrossRef]